RSC Advances

ROYAL SOCIETY OF CHEMISTRY

www.rsc.org/advances

Fabrication and characterization of silk fibroin/chitosan/Nano γ-alumina composite scaffolds for tissue engineering applications

Abbas Teimouri[a,*], Raheleh Ebrahimi[a], Alireza Najafi Chermahini,[b] Rahmatollah Emadi[c]

[a] *Chemistry Department, Payame Noor University, 19395-3697, Tehran, I. R. of Iran*
[b] *Department of Chemistry, Isfahan University of Technology, Isfahan, 841543111, Iran*
[c] *Department of Materials Engineering, Isfahan University of Technology, Isfahan 84156-83111, Iran*

ABSTRACT

A series of silk fibroin/chitosan/Nano γ-alumina composite scaffolds have been prepared using the lyophilization technique for tissue engineering. These were then characterized using SEM, XRD, EDX, FTIR and TGA. In addition, the water uptake capacity, degradability, and biomineralization capability of the composite scaffolds were assessed. The inclusion of γ-alumina in the SF/CS γ-alumina scaffolds was found to result in increased compressive strength and water uptake capacity and decreased porosity. Cytocompatibility of the scaffolds was also assessed by MTT assay and cell attachment studies using Human Gingival Fibroblast cells (HGF, NCBI: C-131). Results showed no signs of toxicity and cells were found attached to the pore walls within the scaffolds. These results proposed that the developed composite scaffolds meet the requirements for tissue engineering applications.

Keywords: silk fibroin; chitosan; tissue engineering; microporous materials.

1. Introduction

[*]Corresponding author at: Department of Chemistry, Payame Noor University (PNU), Isfahan, P.O. Box 81395-671, Iran. Tel.: +98 31 33521804; fax: +98 31 33521802.
E-mail addresses: a teimouri@pnu.ac.ir, a teimoory@yahoo.com (A. Teimouri).

Tissue engineering has recently developed as a new method used in the fabrication of functional new tissue to replace damaged tissue [1-3]. The process generally involves isolating specific cells and then allowing them to grow on or within a scaffold. The scaffolds are however expected to possess certain advantageous characteristics such as an interconnected porous structure with sufficiently large pore sizes to allow cell-growth within the pores. In addition, they should be biodegradable or bioresorbable, to ensure replacement of the scaffold by the tissue, and also possess suitable mechanical properties compatible with intended site of implantation[4]. Scaffold materials can be natural or synthetic, degradable or nondegradable, depending on the offered use [5]. A variety of materials have been created which possess such suitable characteristics, some of which include polymers, ceramics and metals, or sometimes even a composite of these materials [6, 7]. Ceramics, including alumina, zirconia, calcium phosphate and bioglass, are mostly used for hard tissue engineering while the most generally used natural polymers in tissue engineering are fibroin, chitosan, gelatin, alginate, collagen and hyaluronic acid [8]. Silk fibroin is an insoluble protein containing up to 90% of the amino acids glycine, alanine, and serine that form crystalline β-pleated sheets in silk fibers [9]. Silk has been explored for an extended variety of biomaterial applications involving fibroblast and osteoblast cell support matrixes and also for ligament tissue engineering [10, 11]. However, the poor mechanical strength of porous SF scaffolds makes them unsuitable for hard tissue engineering. There is therefore need to improve them in this regard, by incorporating other natural or synthetic polymers, such as chitosan, collagen and poly(vinyl alcohol) (PVA) so forth [12–16]. Chitosan is the N-deacetylated form of chitin obtained by treatment of the latter with a strongly basic solution and is a widely used natural cationic polymer in biomedicine [17]. It is biodegradable and non-toxic and in addition has a hydrophilic surface which promotes cell adhesion and proliferation[18, 19]. Several kinds of bioceramics have been considered for treating damaged and diseased bones with particular emphasis on the bioinert ceramics (e.g.

alumina and zirconia) [20, 21]. Among the oxides used for the making of porous ceramics, alumina is of particular importance. Alumina (Al_2O_3) is a biocompatible bioinert ceramic is well known as potential engineering ceramic [22, 23]. The use of alumina as scaffold could be due to its high mechanical strength, minimum wearing, chemical stability, biocompatibility and biostability. Porous alumina ceramics has been coated with bioactive coatings such as bioactive glass [24] and calcium phosphate [25] as well as hydroxyapatite [26, 27] It has been informed that alumina/hydroxyapatite (HA) scaffolds can initially allow cell adhesion and growth [28]. Yang etal. [29] indicated that nanoporous alumina could be used for tissue engineering. Substantial cell-attachment and growth on alumina substrates has also been presented by Chanda et al. [30] Recently, Al_2O_3/calcium silicate composite has been successfully fabricated [31]. Sopyan, etal. [32] carried out experimental studies on porous alumina–HA composite.

In continuation of our previous studies on the construction of composite scaffolds [33, 34], we focus, in the present study, on the preparation, characterization, bioactivity and biodegradation of nanocomposite scaffolds silk/chitosan/Nano γ-alumina in detail. The effect of different amounts of γ-alumina powders on the structure, strength and hydrophilicity of the fabricated composite scaffolds were examined too.

Experimental section

Materials and Instruments

Good quality raw cocoons of the silkworm, *Bombyx mori,* were purchased from a silk Company (Rasht, Iran). Distilled water was used in the preparation of the aqueous silk fibroin solution. Cellulose dialysis cassettes (Slide-A-lyzer, MWCO 12000 Da (Sigma)) were used to eliminate impurities from silk fibroin solution. Na_2CO_3, LiBr and methanol were provided by

Merck. Chitosan (CS) powder (low molecular weight, 75–85% deacetylated), and alumina (γ -Al_2O_3) powder (<100 nm) and DMSO were provided by Sigma–Aldrich, USA. Acetic acid 100% and 25% aqueous solution glutaraldehyde were procured from Merck. 3-(4,5-dimethyhiazol-2-yl)- 2,5-diphenyltetrazolium bromide MTT, Trypsin–EDTA and Foetal bovine serum (FBS), penicillin/streptomycin, RPMI-1640 (GIBCO 51800-035) and Human Gingival Fibroblast cells (HGF, NCBI: C-131) were obtained from Cell Bank, Pasteur Institute of Tehran. All other chemicals were of analytical or pharmaceutical grade and purchased from Sigma-Aldrich or Merck.

Preparation of regenerated fibroin solution

Silk fibroin (SF) was obtained from the silk cocoons according to the previously described protocol with some modifications [33, 35]. The cocoons were boiled several times, for 30 min each time, in an aqueous solution of Na_2CO_3 (0.02 M) to remove the sericin proteins after which the remaining fibroin was dried. The degummed silk fibers were then dissolved in LiBr (9.3 M) and then the resulting solution was dialyzed against distilled water for 3 days using a Slide-A-Lyzer dialysis cassette at room temperature to remove the salt. The undissolved particles were subsequently separated by centrifugation. The final fibroin solution concentration was about 2.5% (w/w), as determined by weighing the remaining solid obtained from a known volume of solution after drying at 60°C for 1 day.

Fabrication of silk/chitosan

Chitosan solution was prepared by dissolving 2 wt.% of chitosan in 0.5 M acetic acid and stirring for 6 h. 2.5 wt.% of silk fibroin was added to prepare a mixture of silk fibroin and chitosan. The two-component mixture was stirred for 2h for uniform mixing. The mixed solution was placed in 24-well polystyrene culture plates, and frozen at −20 °C prior

lyophilized at −20 °C for 48 h. The samples were removed from the molds and etched with methanol for 30 min. After removal of the methanol by evaporation at room temperature, the scaffolds were rinsed four times in deionized water. Finally, the samples were dried and stored in a refrigerated desiccator until used.

Preparation of silk/chitosan/Nano γ-alumina composite scaffold

The silk/chitosan/Nano γ-alumina composite scaffold was prepared by freeze drying. This was done by dissolving the chitosan 2% (w/v) was dissolved in 1% acetic acid solution and then stirring for 3–4 h. The 2.5 % silk fibroin solution was then added into the above chitosan solution and the mixture stirred for another 3–4 h. This was then followed by addition of 0.25% (v/v) glutaraldehyde in a 1:32 ratio (2 h), for crosslinking. This process of cross-linkage of the chitosan with glutaraldehyde takes place through a reaction between the amine groups on the chitosan and the carbonyl groups of glutaraldehyde. Upon obtaining a homogenous mixture, 1 wt% Nano γ-alumina was added to solution and followed by stirring for an additional 3–4 h to disperse the γ-alumina throughout the solution. The resultant solution after γ-alumina addition was then frozen overnight at −80 °C and then freeze-dried in a lyophilizer for 24 h.

Characterizations

The structural morphology of the samples was evaluated by scanning electron microscopy (SEM) using a Philips XL30 operating at an accelerating voltage of 20 kV and qualitative EDX capabilities. The samples were analyzed by X-ray diffraction (XRD) using a Philips X'PERT MPD X-ray Diffractometer (XRD) with Cu Kα radiation (λ=0.154056 nm). The XRD patterns were recorded in the 2θ range of 10–100° (a step size of 0.04° and a time per step of 1s). FTIR spectra were recorded with an JASCO FT/IR-680 PLUS spectrometer

using KBr pellets. To evaluate the weight loss of the SF/CS/ Nano γ-alumina composite scaffold during thermogravimetric (TG) analysis, a test was performed using a Dupont TGA 951 at temperatures ranging from room temperature to 1000 °C in the air and at a heating rate of 10 °C/min.

Porosity and water-uptake capacity

The porosity of a sample is the fraction of void space within the said sample. The porosity of the SF/CS/Nano γ-alumina scaffolds was measured by the liquid displacement method [36]. The Scaffolds were placed in a 10 ml cylinder containing a defined volume of hexane (V_1). The volume of hexane after inclusion of the scaffold was recorded as (V_2) and acquired after the scaffold had been immersed in hexane for 1 h. The volume difference (V_2-V_1) was the volume of the composite scaffold. The volume of the hexane remaining in the cylinder after the removal of the scaffold was recorded as (V_3). The quantity (V_1-V_3), volume of hexane within the scaffold, was determined as the void volume of the scaffold. The total volume of the scaffold was $V = (V_2-V_1) + (V_1-V_3) = V_2-V_3$. The porosity of the scaffold was obtained by the following equation:

Porosity (%) = $(V_1-V_3) / (V_2-V_3) \times 100$.

Furthermore, the scaffolds were immersed in distilled water to determine the percentage water uptake. The scaffolds were kept in water at ambient temperature for 48 h to ensure water impregnation into the open pores. The water uptake of the porous scaffolds was calculated as water-uptake (%) = (Ww –Wd)/Wd × 100, where Ww and Wd represent the wet weight of the scaffold and initial dry weight sponge, respectively. Water-uptake was expressed as mean±SD (n = 3).

In vitro bio-degradation

The biodegradation test of the porous scaffold was studied in phosphate buffer saline (PBS) medium containing lysozyme at 37 °C for a time period of 7, 14, 21 and 28 days. This was done by soaking the samples in PBS solution for different time lengths after which the samples were dried. Dry scaffolds were weighed and immersed in PBS and incubated at 37 °C for three different time intervals that is 24 h, 48 h and 72 h. The degradation percentage was determined by the formula: Degradation % = $[(W_i - W_t) / (W_i)] \times 100$, where (W_i) is the initial dry weight of the construct and the dry weights of the scaffolds are noted as (W_t). Degradation rate was recorded as mean±SD (n = 3).

In vitro bio mineralization

This section of the study was carried out using the standard in vitro procedure described by Kokubo et al.[37]. The composite scaffolds were soaked in simulated body fluid SBF (pH 7.40) at 37 °C in a closed Falcon tube for 7 and 14 days. After the specified time, the scaffolds were washed three times with deionized water to remove any adsorbed minerals. The scaffolds were then lyophilized and sectioned and subsequently evaluated by FTIR, XRD and SEM for mineralization.

Mechanical properties

The compressive strength were tested for SF, CS, SF/CS and SF/CS/Nano γ-alumina 90:5:5, 80:10:10 and 70:15:15 scaffolds using the Universal Testing Machine (Hounsfield-H25KS) by applying compressive pressure at a rate of 0.5 mm/min at a room temperature using a 0.2 kN load cell. Cylindrical shaped scaffolds measuring 15 mm (diameter) by 14.4 mm (height) were used for the tests, according to a modified procedure based on the ASTM method F451-95. Three parallel samples were tested for every scaffold and the mean compressive strength value of different scaffolds was taken. The average data of the test

results were plotted and the elastic modulus was calculated as the slope of the initial linear portion.

MTT assay

The MTT assay was developed for cell viability and mitochondrial activity assessment. Living cells reduce the MTT substrate (3-[4,5-dimethylthiazol-2-yl]-2, 5-diphenyltetrasodium bromide) to a dark-blue formazan in the presence of active mitochondria and thus an accurate measure of mitochondrial activity of cells in a culture could be carried out. 2×10^5 cells were seeded in the scaffolds and cultured in 24- well plates for 24, 48 and 72 hours. The same number of cells was cultured in wells without the scaffold as the control group. Briefly, exhausted media was removed, replaced with media containing 400 µl fresh culture and 40 µl MTT solution (MTT, Sigma, USA) (5 mg ml^{-1}) in each well, followed by incubation for 4 h at 37 °C. After incubation, 400 µl of dimethyl sulfoxide (Sigma, USA) was added to dissolve the blue formazan crystals and 100 µl of the solution transferred to 96 -well plate and absorbance was measured at 570 nm in an ELISA reader (Hyperion MPR4).

To observe adhesion and morphologies of the cells attached to scaffolds, the cells were rinsed with PBS and then soaking in 2.5% glutaraldehyde in PBS solution for 1 h at room temperature. After thorough washing with PBS, the cells were dehydrated in a graded series of ethanol aqueous solutions (70–100%) and drying in vacuum at room temperature. Before SEM observation, the samples were coated with very thin layer of gold.

Results and discussion

Methanol treatment results

The SF was transformed from a random coil structure into a β-sheet conformation when treated with methanol [38]. The molecular conformation of the SF was then studied using

spectroscopy to determine the nature of the transformation (Fig. 1A). Shift of absorption peaks in FT-IR spectra confirms the transformation of silk fibroin from a random coil structure to a β-sheet conformation in the amide I and II regions. In Figure 1A (a), the peaks of fibroin before methanol treatment were positioned at 1638 cm^{-1} (amide I) and 1549 cm^{-1} (amide II), and they were attributed to the random coil conformation. After methanol treatment [Figure 1A (b)], characteristic peaks showed bands associated with the β-sheet conformation were seen at 1634 cm^{-1} (amide I) and 1541 cm^{-1} (amide II) [39].

X-ray diffraction patterns of SF before and after methanol treatment are shown in Figure 1B. Before methanol treatment [Figure 1B (a)], XRD showed two strong peaks around 2θ= 14° and 16.5° representing silk I structure [39] for extracted fibroin. After methanol treatment [Figure 1B (b)], those peaks shifted to 2θ=20° and 21°, respectively, also indicating a conformational change from silk I to silk II [39-41].

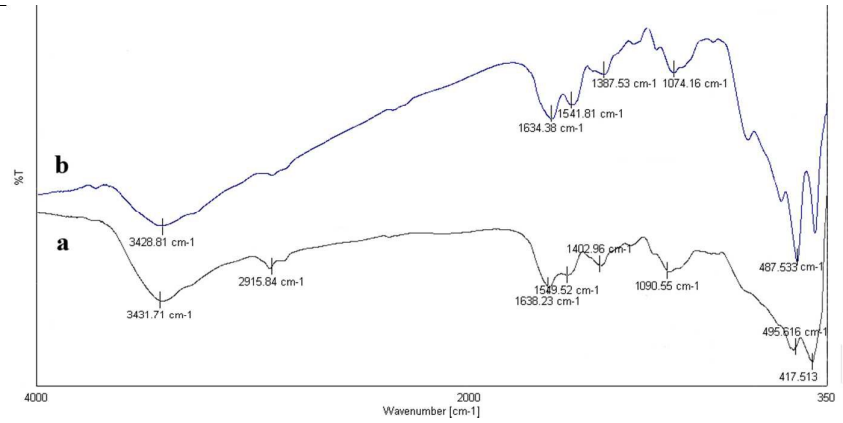

A

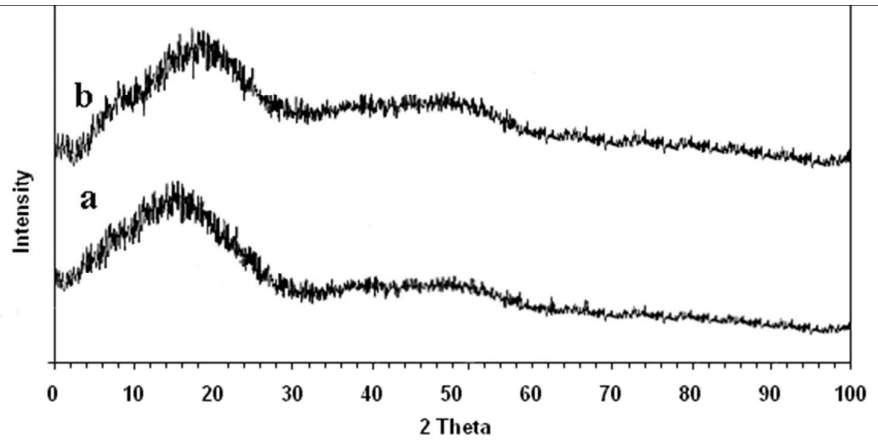

B

Fig. 1. A) FT-IR spectra of fibroin before (a) and after (b) methanol treatment. B) XRD pattern of fibroin before (a) and after (b) methanol treatment.

FT-IR analyses of the SF/CS/Nano γ-alumina composites

Figure 2 shows the FTIR spectra of the samples in the spectral range of 400–4000 cm^{-1}. The pure silk fibroin showed absorption bands at 1658 cm^{-1} (amide I) and 1530 cm^{-1} (amide II), which were attributed to a random coil. [34] The band at 3437 cm^{-1} in samples corresponds to –OH stretching vibration. Although there is a possibility of overlapping between $–NH_2$ and –OH stretching vibrations, the band 3437 cm^{-1} corresponds to –OH and $–NH_2$ stretching vibrations. The band at 1633 cm^{-1} corresponds to amide stretching vibration. The bands at 2926 and 1411 cm^{-1} corresponds to aliphatic stretching vibrations of –CH and –NH bending respectively. On the other hand, absorption bands at 1155 and 900 cm^{-1}, which were assigned to the saccharide structure. FTIR spectra of SF/CS/ γ-alumina scaffolds showed peaks at 1633 cm^{-1} and 1078 cm^{-1} which correspond to the primary amide groups of Silk and C–O stretching of chitosan, respectively. [42]

The broad bands that appear in the range of 500–1000 cm^{-1} could be characteristic vibrations of aluminium oxide. The broad band at 665 and 845 cm^{-1} can be assigned to bending mode of O–Al–O and Al–O stretching mode, respectively.

XRD analyses of the SF/CS/Nano γ-alumina composites

The XRD spectrum of SF/CS displayed in Fig. 3 (a) revealed that it had low crystallinity. On the other hand, the XRD spectrum of γ-alumina shown in Fig. 3 (b) showed peaks at 34°, 46° and 51.10° which are specific to γ-alumina [43]. The XRD studies on SF/CS/ γ-alumina shown in Fig. 3 (c) showed the characteristic peaks for both chitosan (2θ=9.3°, 19.7° and 22.5°) and silk fibroin (2θ=8.9° and 21.8°) suggesting the presence of both in the scaffold. Furthermore, the sharp peak seen in the XRD of the composite at 66° could be due to the dominating nature of γ-alumina over the amorphous nature of Silk/chitosan 70:15:15, 80:10:10 and 90:5:5. The intensity of peaks increased along with the increase of γ-alumina content in the composite scaffolds accompanied with other characteristic peaks of Silk/chitosan. The peaks for the presence of 15 wt.% γ-alumina in Silk/chitosan/γ-alumina 70:15:15 nanocomposite were observed more intensively than 80:10:10 and 90:5:5 Silk/chitosan/γ-alumina nanocomposite.

12

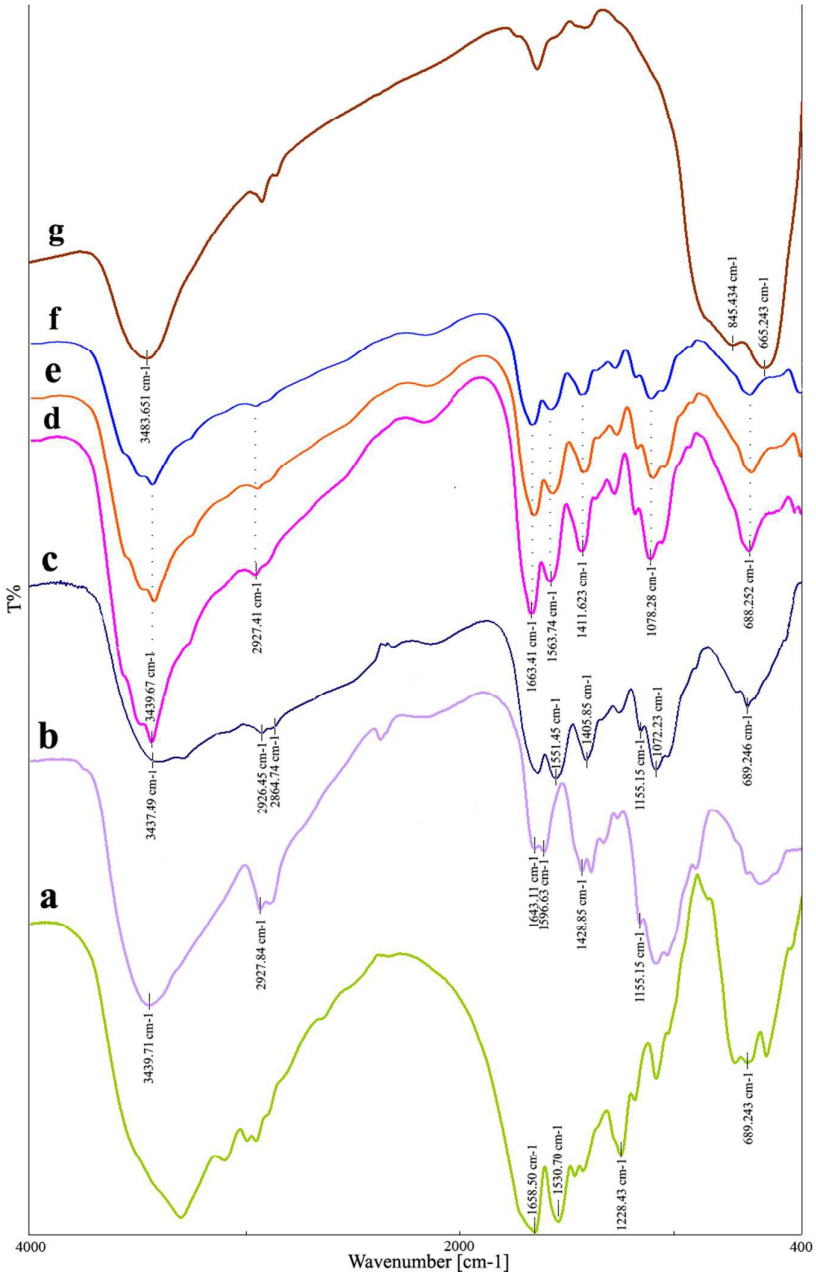

Fig 2. FTIR spectra of (a) SF, (b) CS, (c) SF/CS, (d) SF/CS/Nano γ-alumina 70:15:15, (e) SF/CS/Nano γ-alumina 80:10:10, (f) SF/CS/Nano γ-alumina 90:5:5, (g) Nano γ-alumina

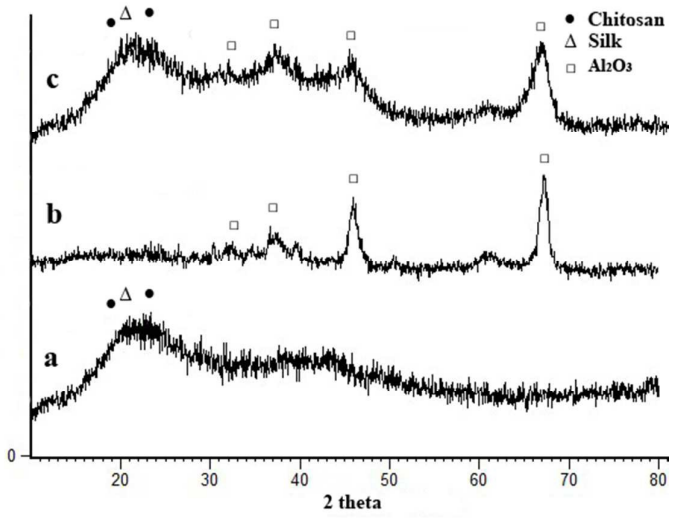

Fig. 3. XRD spectrum: (a) SF/CS, (b) Nano γ-alumina, (c) SF/CS/Nano γ-alumina 70:15:15, (d) SF/CS/Nano γ-alumina 80:10:10, (e) SF/CS/Nano γ-alumina 90:5:5

SEM analysis

For the investigation of the surface structure and size of pores, a scanning electron microscope (SEM) was used. The microstructure of a scaffold has a significant influence on cell proliferation and migration, all of which are key issues in tissue engineering. Sufficient pore sizes and interconnectivity of pores are necessary factors for nutrient and oxygen transport to the cells. The ideal pore size range for tissue engineering scaffolds has been found to be between 150–200 μm as reported earlier [44, 45], Fig. 4 shows SEM micrographs of the pure SF, γ-alumina, SF/CS and SF/CS/Nano γ-alumina. The pure SF scaffold showed a macroporous structure with interconnected open pores and pore sizes varying from 100 to 200 μm (Fig. 4a). The SEM image of γ-alumina is illustrated in (Fig. 4b). Also, as shown in (Fig. 4c), SF/CS had a homogeneous porous structure, with a pore size range from 100 to 300 μm. The blended SF/CS scaffolds showed greater pore sizes when compared to the pure silk fibroin. Additionally, similar internal structure morphologies as in the SF and SF/CS scaffolds were observed as well in the SF/CS/ γ-alumina scaffolds. However, the morphologies on the surface of the pore walls were quite different in both the pure SF

scaffold and the composite scaffolds. A comparison of the cross-section of the silk fibroin and SF/CS, shows that the pores in SF/CS are more interconnected than the pores in silk fibroin and this may be due to the hydrophilicity of the chitosan. However, the morphologies on the surface of pore walls between the pure SF scaffold and the composite scaffolds were quite different. These results give a view into the porous structure of the scaffold and the distribution of the pores. There was decrease in the pore size with the increase of γ-alumina content in the blends. The blended scaffolds having high γ-alumina content show smaller pore size as compared to SF/CS scaffolds. This indicated that with addition of γ-alumina, the pore size got reduced. However the SF/CS/Nano γ-alumina 70:15:15 scaffold (Fig. 4d) showed that several pores are interconnected and decrease in pore size, which ranged from 50 to 150 μm, a range best suited for cell growth. The EDX results showed the presence of the characteristic elements of the materials used. (Figs. 4c-e)

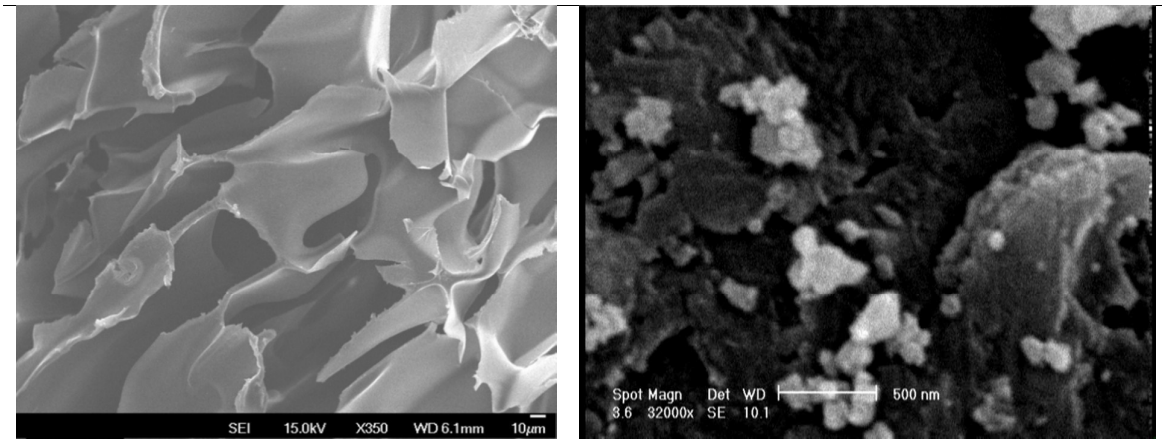

a **b**

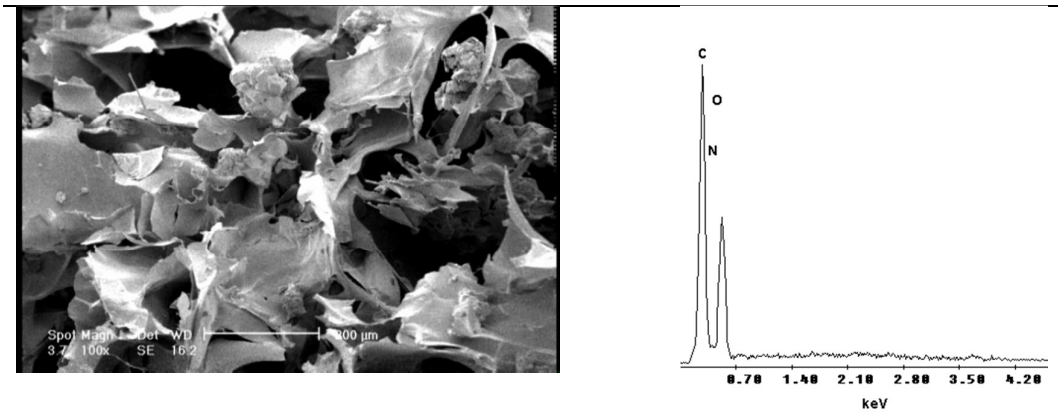

c

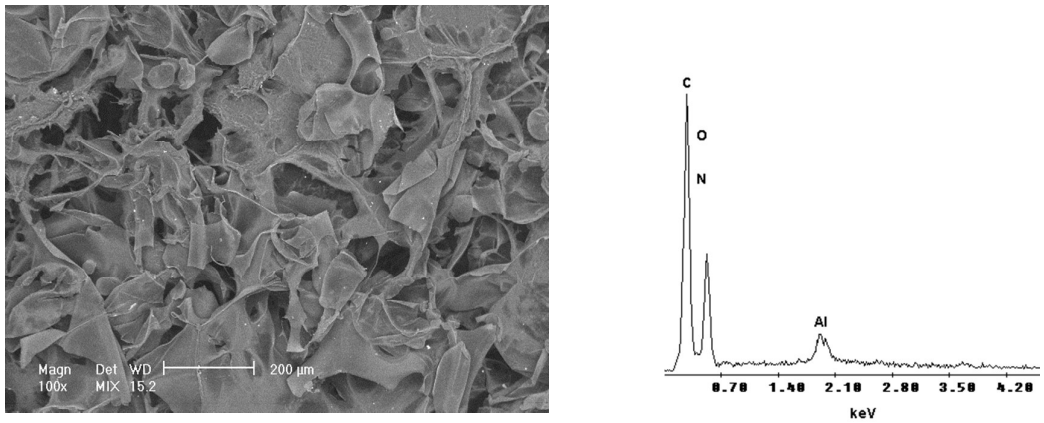

d

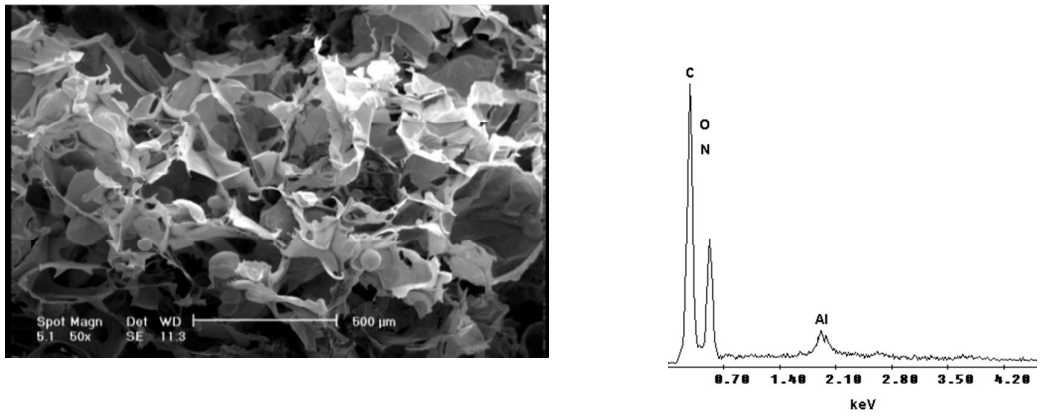

e

Fig 4. SEM images of the (a) pure SF, (b) Nano γ-alumina, SEM images and EDX analysis of (c) SF/CS, (d) SF/CS/Nano γ-alumina 70:15:15, (e) SF/CS/Nano γ-alumina 80:10:10.

Thermal degradation of SF/CS/Nano γ-alumina

Thermal degradation of the scaffolds was studied using TGA (Fig. 5). As shown in Fig. 5, the pure SF began to decompose at about 270 °C and had decomposed completely by the time the temperature rose to 500 °C. The thermal degradation process was divided into two stages. The first one in the case of both the scaffolds, which started from 53-200 °C, can be related to the loss of adsorbed water. During the second stage (700-1000 °C) a slight difference in weight loss was noted, which confirmed the degradation of the sample as a result of the release of bound water and breaking of bonds in the sample core. At this stage the breaking of peptide bonds in the sample core led to the depolymerization of the silk fibroin. A slower degradation rate prominent for the SF/CS/Nano γ-alumina 70:15:15 composite scaffold was observed in comparison to the SF/CS, which could be due to the incorporation of γ-alumina into the scaffolds.

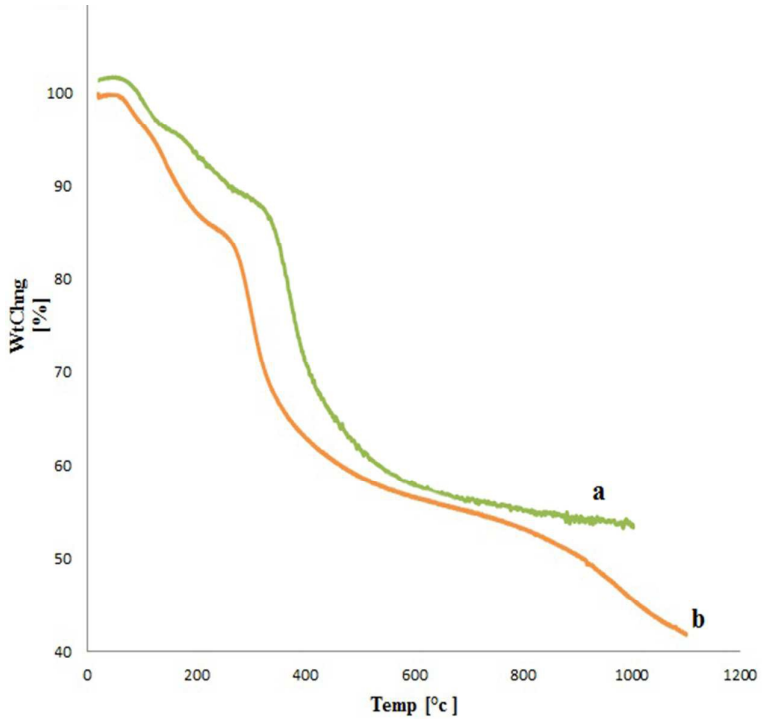

Fig. 5. TG profiles of (A) SF/CS, (B) SF/CS/Nano γ-alumina 70:15:15

Porosity and water-uptake capacity

Porosity is an important factor for the application of scaffolds in cell culture applications [46, 47]. In order to accommodate a larger number of cells, the scaffolds need to be highly porous with higher surface to volume ratios, so that there is provision for sufficient area for cell growth and attachment. Scaffolds with high porosity meet mass-transport requirements for cell nutrition. The diffusion rate of nutrients and waste materials are enhanced and porous channels help in cell migration and cell attachment [48]. The measured water-uptake capacity and pore sizes of the SF, CS, SF/CS and SF/CS/Nano γ-alumina 70:15:15, 80:10:10, 90:5:5 composite scaffolds are presented in Table 1, and the percentage porosities of the SF, CS, SF/CS and SF/CS/Nano γ-alumina 70:15:15, 80:10:10, 90:5:5 composite scaffolds are presented in (Table 1 and fig 6a). Result (fig 6b) shows that the addition of alumina decreased the swelling of SF/CS/Nano γ-alumina scaffolds. This may be due because alumina formed cross-link between the chains and decreased the hydrophilicity of silk and chitosan.

Table 1 Characteristics of SF/CS/Nano γ-alumina composite scaffold.

Composites	Pore size (μm)	Porosity (%)	Water uptake capacity (%)
SF	122±34	91.6±2.3	572±22
CS	90±26	65±1.5	130±39
SF/CS	155±42	87±3.08	1258±209
SF/CS/Nano γ-alumina 70:15:15	135±28	80±2.01	2111±785.59
SF/CS/Nano γ-alumina 80:10:10	140±16	83±1.21	1946±56
SF/CS/Nano γ-alumina 90: 5: 5	148±22	86±2.51	1138±102

In vitro biodegradation studies

The *in vitro* degradation behavior of SF/CS/Nano γ-alumina 70:15:15 scaffolds was studied by immersion in PBS solution (Fig. 6c) and PBS-lysozyme solution (Fig. 6d), for a

period of 4 weeks. The degradation rate of SF/CS/Nano γ-alumina scaffold was seen to increase with the passage of time. The results of the degradation showed that the introduction of γ-alumina powder into the scaffolds had an effect on the observed weight loss. The degradation rate of chitosan is fast, this could be attributed to an increase in hydrophilicity of the composite. The addition of silk fibroin could delay the biodegradability of scaffolds. The incorporation of alumina significantly reduced the degradation rate with around 60% of SF/CS/Nano γ-alumina still remaining after 28 days of incubation in lysozyme. By the end of one week, the SF/CS/Nano γ-alumina had degraded by about 20% and this gradually increased up to 41% by day 28. This shows that the material undergoes controlled biodegradation which is desirable for tissue engineering applications.

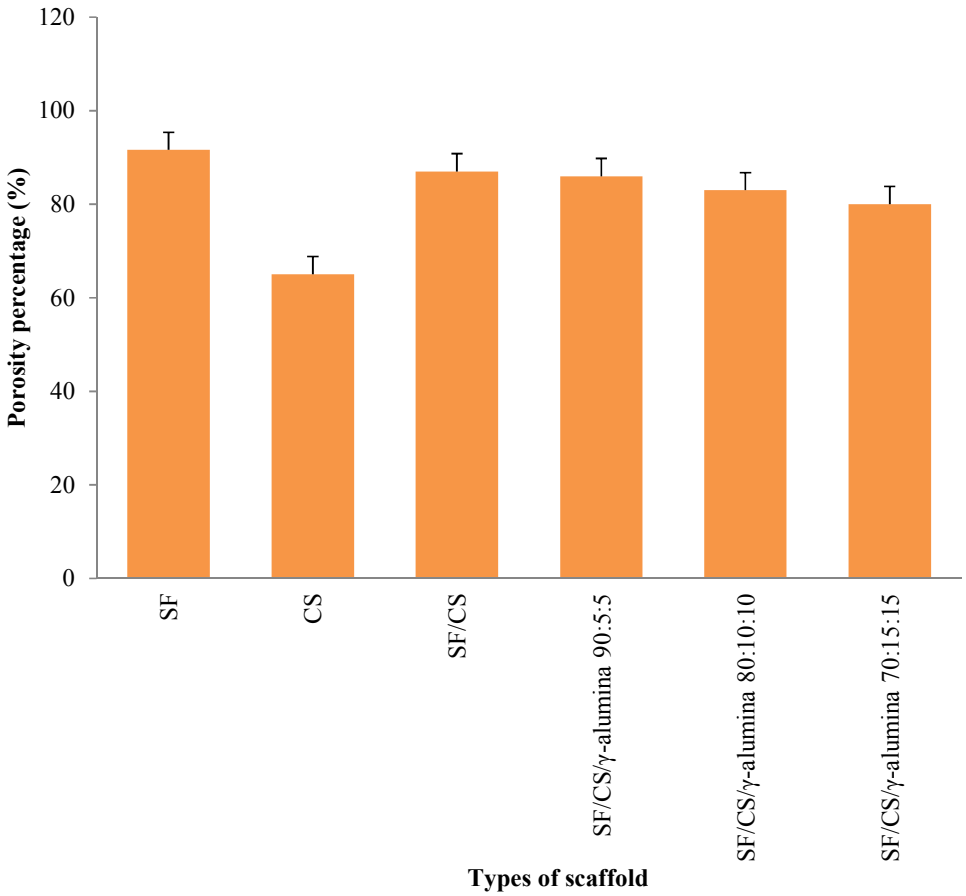

a

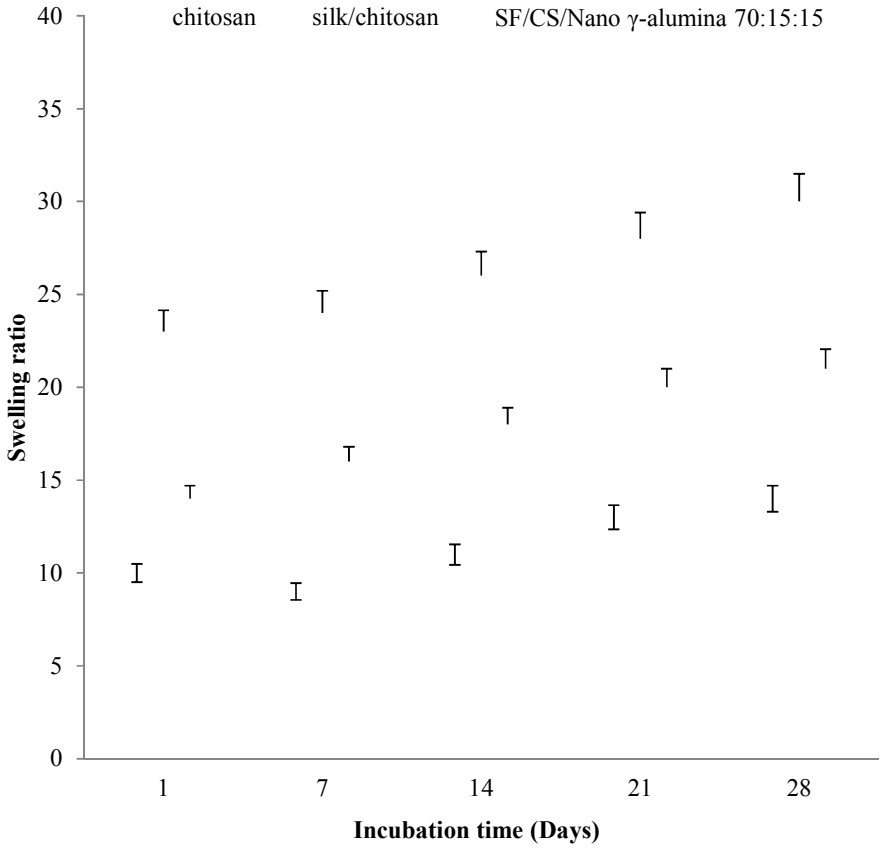

b

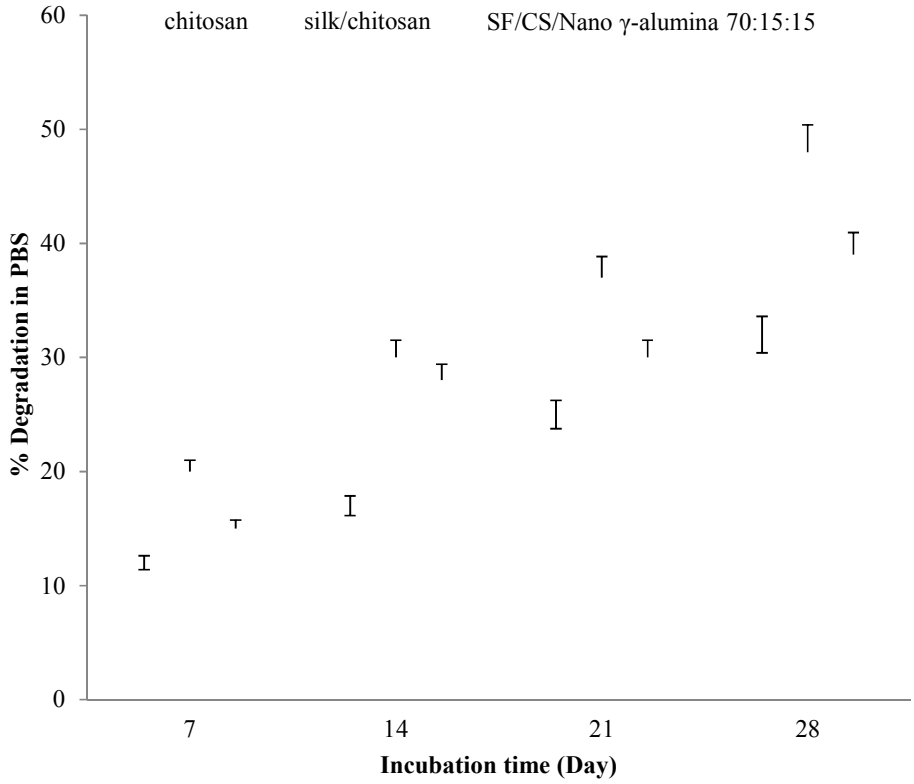

c

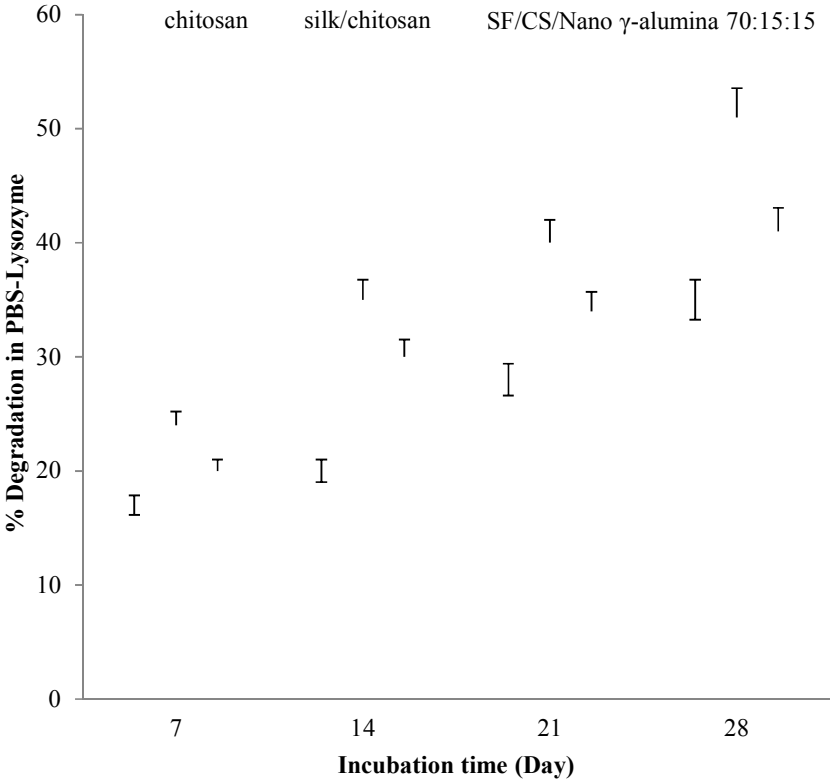

d

Fig. 6. a) Porosity percentage of pure SF, pure CS, SF/CS and SF/CS/Nano γ-alumina 90:5:5, 80:10:10, 70:15:15, b) swelling study of pure CS, SF/CS, SF/CS/Nano γ-alumina 70:15:15 and degradation behavior of pure CS, SF/CS, SF/CS/Nano γ-alumina 70:15:15 scaffolds in: c) PBS solution and d) PBS-Lysozyme solution.

In vitro biomineralization studies

In vitro biomineralization studies were also performed on the SF/CS/Nano γ-alumina 70:15:15 scaffolds by incubating them for 14 days in simulated body fluid (SBF) after which they were analyzed by FTIR, XRD and SEM. The FTIR spectra displayed in Fig. 7 showed bands at 1156 cm^{-1} and 1077 cm^{-1} which are attributed to the P–O stretching and vibration modes while the bands at 502 cm^{-1} and 580 cm^{-1} were assigned to the O–P–O bending mode [50, 51]. The absorption peaks at 727 cm^{-1} and 1447 cm^{-1} corresponding to carbonate (CO_3^{2-}), could be clearly observed in the FT-IR spectra.

Fig. 9 shows the SEM images after incubation and formation of an apatite-like layer can be seen on the surface of the SF/CS/Nano γ-alumina 70:15:15 scaffolds. The present study also indicated that the inclusion of γ-alumina enhanced the biomineralization and bioactivity of the SF/CS/Nano γ-alumina 70:15:15scaffold. These results further confirmed that a bone-like apatite layer was formed on the surface of the composite scaffolds after soaking in SBF another indication of the suitability of these nanocomposite scaffolds for use as materials in tissue engineering applications.

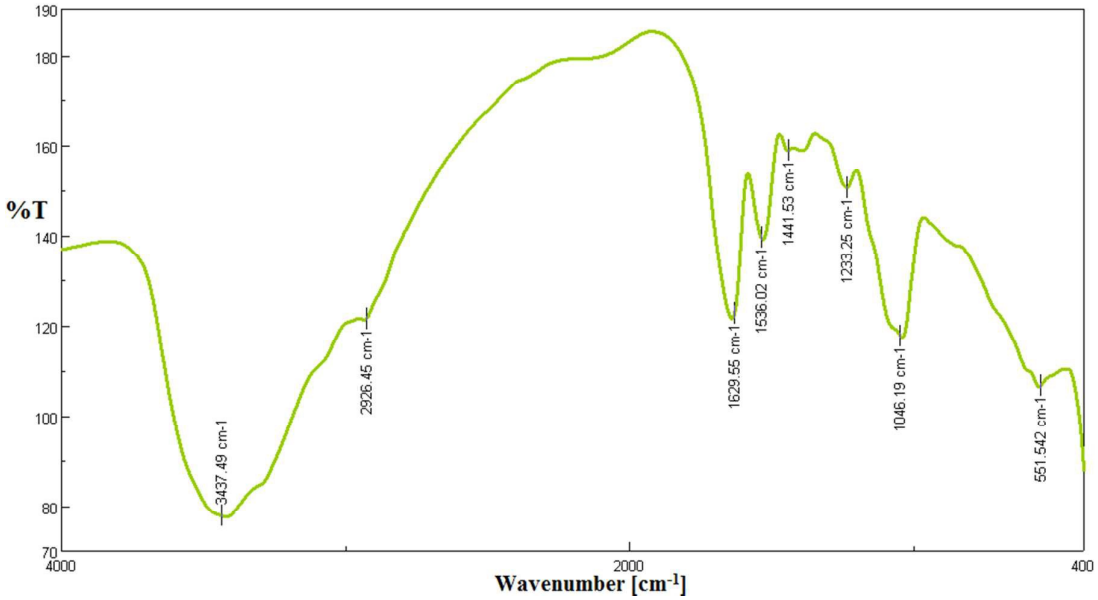

Fig. 7. FTIR of biomineralization of SF/CS/Nano γ-alumina 70:15:15

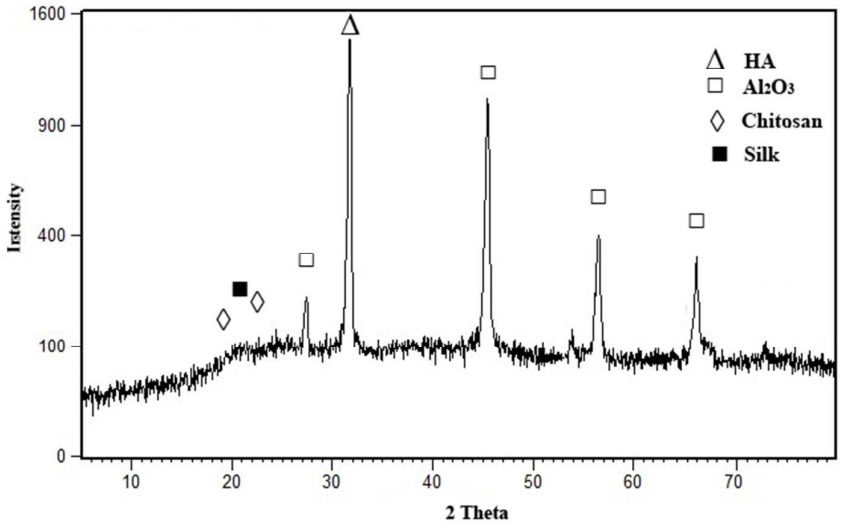

Fig. 8. XRD patterns of SF/CS/Nano γ-alumina 70:15:15 after incubation in SBF.

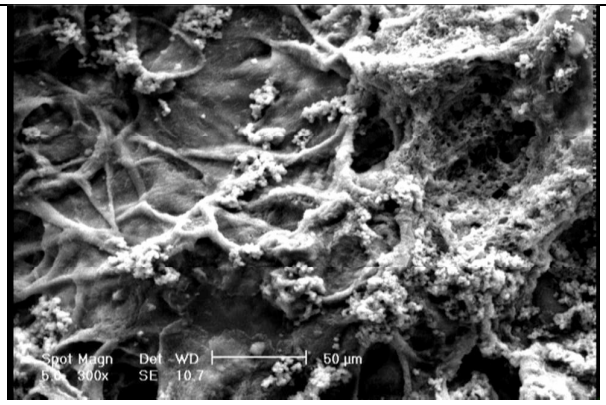

a

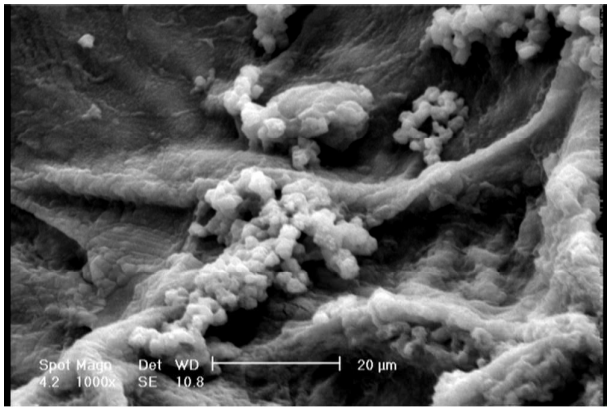

b

Fig. 9. SEM images of apatite formation on SF/CS/Nano γ-alumina 70:15:15 after 14 days.

Mechanical testing

The mechanical properties of matrices have significant effect on cell behaviour such as adhesion, growth and differentiation [51-53]. Mechanical properties of the dry scaffolds have been investigated with a testing machine at room temperature, in a dry state (Fig. 10 a, b), and also in a solution of PBS (Fig. 10c, d). A study of the compressive mechanical properties of the SF/CS and SF/CS/Nano γ-alumina scaffolds were carried out and the results are displayed in (Fig. 10). In this study, the effect of γ-alumina powder on the compressive strength (Fig. 10a, c) and compressive modulus (Fig. 10b, d) of the composite scaffolds was investigated.

As expected, the SF/CS/Nano γ-alumina scaffolds showed improvement in their mechanical strength. The compressive strength and modulus gradually increased when the concentration of γ-alumina was increased. The compressive strength of SF/CS/Nano γ-alumina 70:15:15 was maximum followed by SF/CS/Nano γ-alumina 80:10:10 and 90:5:5 blended scaffolds. A similar trend was observed for the compressive modulus as SF/CS/Nano γ-alumina 70:15:15 also showed significantly higher modulus when compared with the pure silk fibroin, pure chitosan and SF/CS/Nano γ-alumina 80:10:10 and 90:5:5 scaffolds. The compressive strength of the SF/CS scaffold was found to be lower than SF/CS/Nano γ-alumina scaffold. Many other studies have indicated that the decreased pore size and the resultant increase in the thickness of the pore walls could lead to the higher compressive strength and modulus [54, 55]. These results suggest that the inclusion of γ-alumina increased compressive strength of the composite scaffold. It also showed improved mechanical properties when compared to the pure SF/CS scaffold and, as such, was much better suited for tissue engineering applications. The compressive strength was found to have an inverse relationship with the pore size, which could be explained by a decrease in strut strength with increasing the pore size. The decrease in pore sizes and the increase in wall thickness resulting from the inclusion of γ-alumina was responsible for the better mechanical stability in composite scaffolds as compared to the silk fibroin scaffolds. The M. Gibson and Ashby model has generally been applied to relate the modulus to the density of foams [56]. This model is only valid in the elastic field only and is based upon the relation: $E/E_s=C_1 (\rho/\rho_s)^2$, where E is the elastic modulus of the metal foam, E_s is the elastic modulus of the composite, ρ/ρ_s is the relative density, and C_1 is a constant ($C_1 \approx 1$). An increase in the relative density of the structure, improved the Young's modulus. As smaller struts appear denser, they, therefore, have significantly better mechanical properties. According to Gibson and Ashby's model, it has been well documented that the

compressive modulus of composite materials is increased by reducing porosity and including γ-alumina.

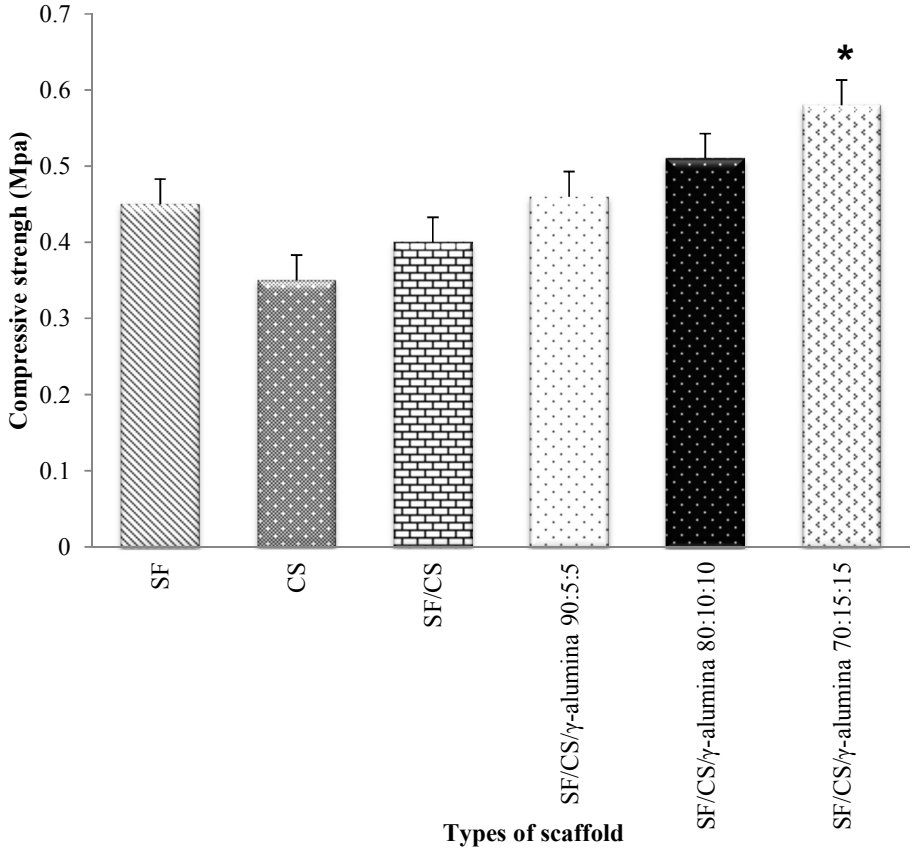

a

26

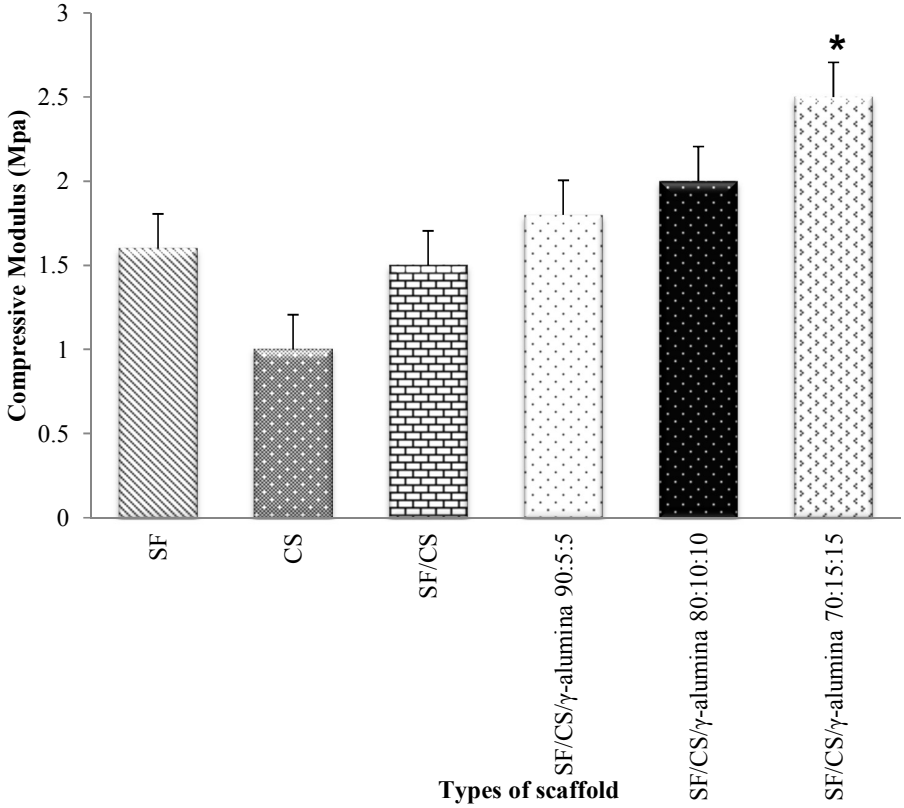

b

27

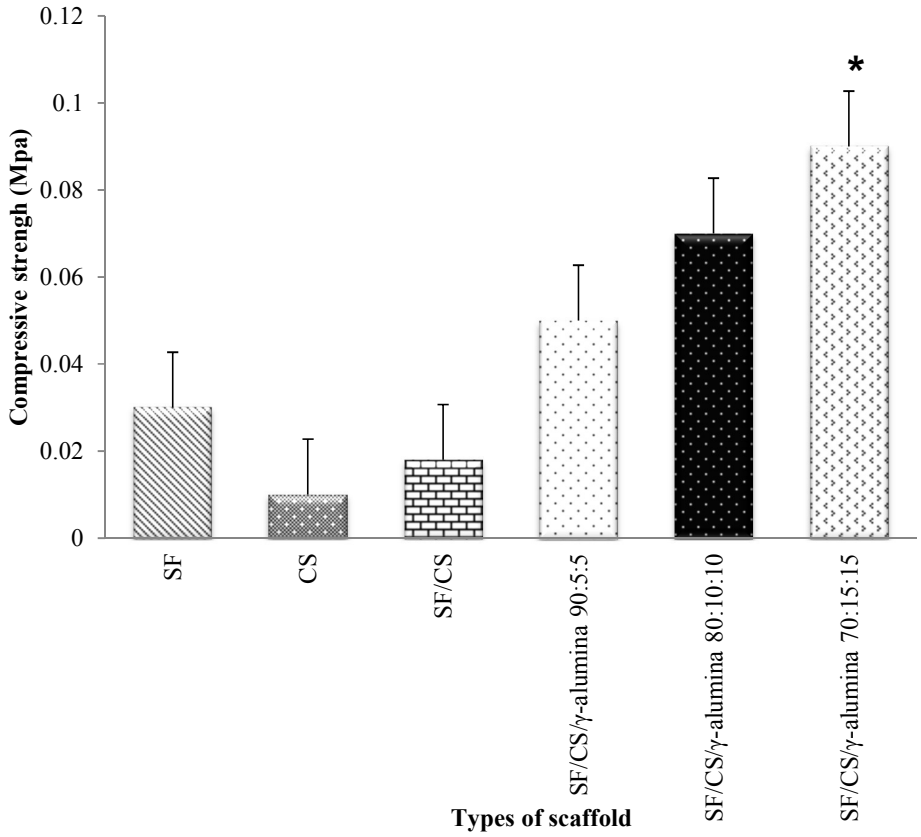

c

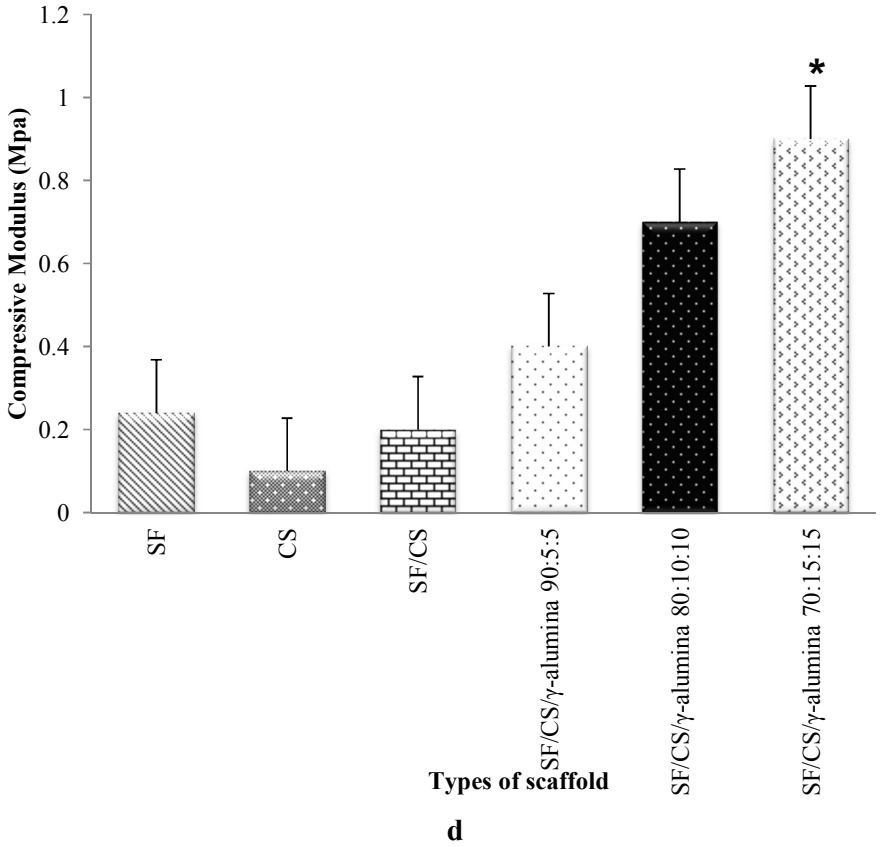

Fig. 10. Mechanical properties of SF, CS, SF/CS and SF/CS/Nano γ-alumina 90:5:5, 80:10:10 and 70:15:15: a) compressive strength; b) compressive modulus, in atmospheric conditions, in a dry state; c) compressive strength; d) compressive modulus, in solution of PBS, pH 7.4, temp. 37 °C. *Significant difference compared to SF/CS scaffolds. Values are mean ± SD (n = 5).

In vitro evaluation of cytotoxicity

Cytocompatibility of the SF/CS/Nano γ-alumina nanocomposite scaffolds was assessed using an MTT assay. As a requirement for the cell growth in vitro, a surface must support cell adhesion and spreading thus proving to be no cytotoxic effect on cell survival and growth. Scaffolds showing higher degree of swelling will have a larger surface area/volume ratio thus allowing the samples to have the maximum probability of cell adhesion into the three-dimensional scaffold as well as maximum cell growth by attachment to the scaffold surfaces.

In this study, the results suggest that there are no significant toxic leachates in the SF/CS/Nano γ-alumina scaffolds after incubation of the cells with the extract containing the

leachates obtained after 24, 48 and 72 h of incubation in the medium. (Fig. 11). There were statistically significant differences between days 1 and 3 for all groups ($p < 0.05$). This obvious increase of the cell numbers with the time supports the compatibility of these scaffolds. No significant increase in cell growth was seen in the control, pure silk fibroin, CS and SF/CS groups after culturing for 72 h due to the space deficiency in the multi-well culture dishes, but the cells related to the composite groups were not like this. From the results it can be concluded that a homogeneous incorporation of Nano γ-alumina into SF/CS scaffold led to higher cell viability compared to that of the SF-only, CS-only scaffold or the SF/CS scaffold blended. The fact that the proliferation of HGF cells is more active within the SF/CS/Nano γ-alumina composite scaffolds might be explained by the formation of appropriate active binding sites for proteins during culture periods thereby resulting in the stimulation of cellular proliferation even more efficiently than the control group. Generally, the scaffolds prepared in this work were seen to possess favorable cell-compatible characteristics and can be considered as suitable materials for tissue engineering applications.

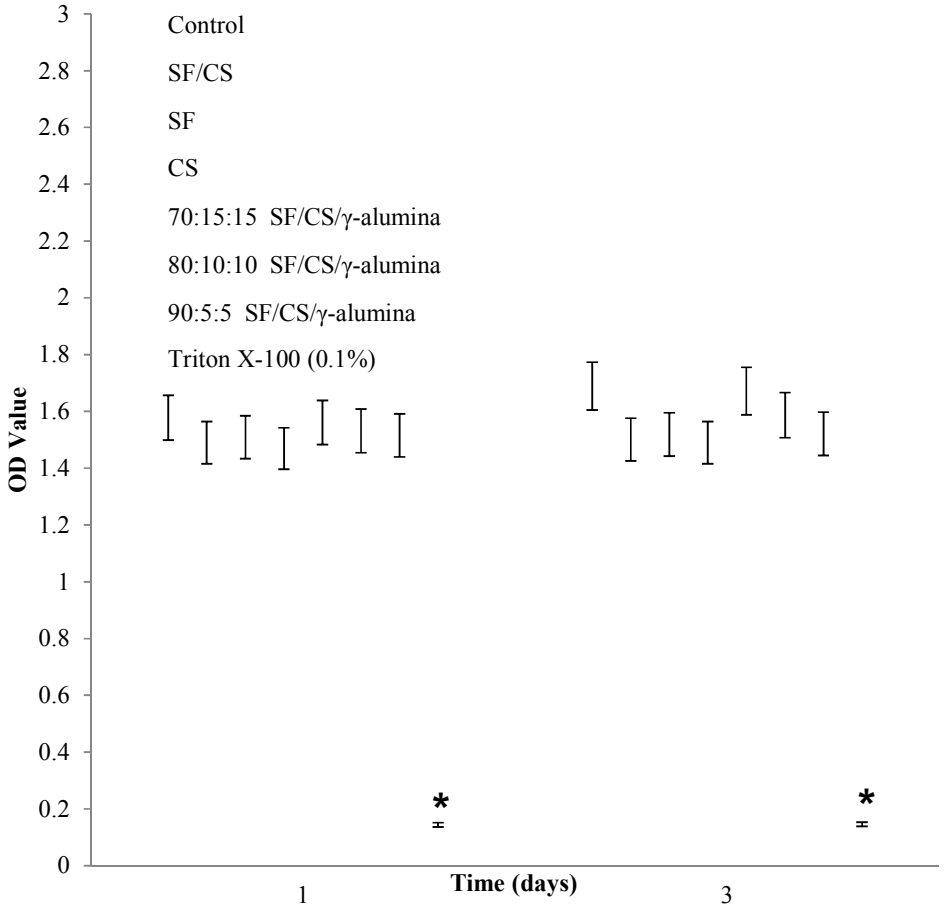

Fig. 11. In vitro cytotoxicity evaluation of HGF cells in contact with scaffolds tracts for different periods of time. *Significantly decreased compared to control. ($p \leq 0.05$).

Figures 12a-c show the photographs of HGF fibroblasts in SF/CS/Nano γ-alumina 70:15:15 scaffolds after 3 days of culturing. These outcomes were not significantly different when compared to the control cultured group. The results show an increase in cell activity in culture media containing SF/CS/Nano γ-alumina 70:15:15 scaffold during incubation, indicating no cytotoxic effect on cell survival and growth. Generally, the scaffolds prepared in this work were seen to possess favorable cell-compatible characteristics and can be considered as efficient materials for tissue engineering applications.

a **b** **c**

Fig. 12. Light microscopy photographs (100×) of the cell viability of HGF cells on SF/CS/Nano γ-alumina 70:15:15 scaffold after cultured for (a) 1 day; (b) 2 days; (c) 3 days.

Cell attachment studies

As a requirement for the cell growth in vitro, a surface must support cell adhesion and spreading thus proving to be no cytotoxic effect on cell survival and growth. SEM images (Fig. 13) were used to study the attachment and morphology of the cells on the scaffolds. SEM images of scaffolds seeded with cells and incubated for 24 h showed that the cells were attached to the scaffolds, demonstrating similar morphology with a flattened appearance on the surface of scaffolds. Cell attachment studies showed that the SF/CS/Nano γ-alumina 70:15:15 scaffold displayed significantly increase in cell attachment, an indication of their suitability for tissue engineering. The higher attachment on SF/CS/Nano γ-alumina 70:15:15 scaffold is believed to be due to the increase in surface area.

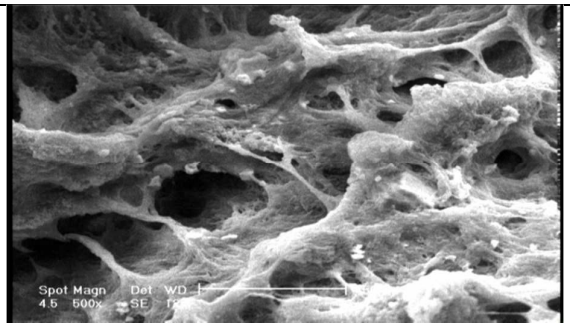

a

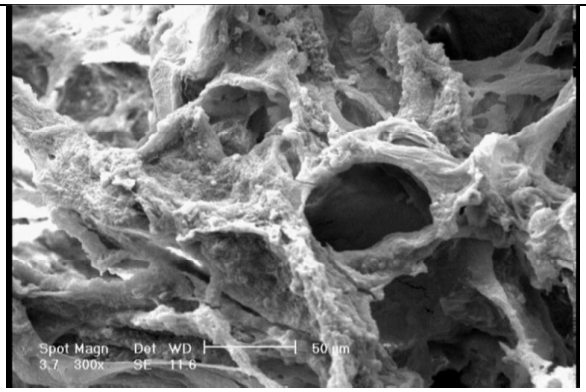

b

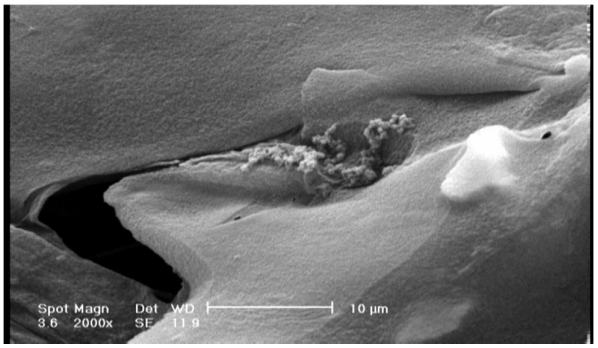

c

Fig. 13. Cell attachment (human gingival fibroblast) on SF/CS/Nano γ-alumina 70:15:15 scaffold represents 500 and 10 µm respectively.

Conflict of interest

The authors declare no competing financial interest.

Conclusions

In tissue engineering, a scaffold should meet several requirements such as porous structure, biocompatibility, controlled biodegradability or bioresorbability. The porous scaffold can be constructed from biodegradable polymers, inorganic materials and their composites. In this study, SF/CS and SF/CS/Nano γ-alumina scaffolds were prepared, characterized and compared. They were found to be porous and biodegradable, both of which

are essential for tissue engineering. The addition of γ-alumina nano powders considerably improved compressive strength, water-uptake capacity and slowed the Thermal degradation in the SF/CS scaffold. Considering the results from FT-IR spectroscopy analysis also showed that γ-alumina and the β-sheet conformation of SF existed in the structure of the scaffolds. Cells seeded onto the SF/CS/Nano γ-alumina scaffold were found to be non-toxic in nature. Thus, it is suggested that SF/CS/Nano γ-alumina composite scaffold would serve as a suitable template for tissue engineering applications.

Acknowledgements

Supports from the Payame Noor University in Isfahan Research Council (Grant # 62370) and contribution from Isfahan University of Technology are gratefully acknowledged. The authors would like to thank Dr. L. Ghorbanian for critical reading of the manuscript.

Notes and references

1 T.C. Flanagan, B. Wilkins, A. Black, S. Jockenhoevel, T.J. Smith and A.S. Pandit, Biomaterials., 2006, 27, 2233–2246.

2 G. Chen, T. Ushida and T. Tateishi, J. Mater Sci Eng C., 2002, 17, 63–69.

3 L.A. Solchaga, V.M. Goldberg and A.I. Caplan,. Clin. Orthop. Relat. Res. S391, 2001, 391, 161-170.

4 D.W. Hutmacher, Biomaterials., 2001, 21, 2529–2543.

5 S. Ramakrishna, J.Mayer, E.Wintermantel, and K.W. Leong, Composites Science and Technology., 2001, 61, 1189–1224,.

6 S.F. Yang, K.F. Leong, Z.H. Du and C.K. Chua, Tissue engineering., 2001, 7, 679-689.

7 G. Ryan, A. Pandit and D.P. Apatsidis, Biomaterials., 2006, 27, 2651-2670.

8 S.V. Dorozhkin, Biomaterials., 2010, 31, 1465-1485.

9 T. Asakura and D.L. Kaplan, Silk Production and Processing. In Encylopedia Agricultural Science, C.J. Arntzen, E.M. Ritter, Eds, Academic Press: New York, 1994, 4, 1-11.

10 S. Sofia, M.B. McCarthy, G. Gronowicz and D.L. Kaplan, J. Biomed. Mater. Res., 2001, 54, 139-148.

11 J. Perez-Rigueiro, C. Viney, J. Llorca and M.J. Elices, Appl. Polym. Sci. 1998, 70, 2439-2447.

12 Guo-Jyun Lai, K.T. Shalumon, Shih-Hsien Chen, Jyh-Ping Chen, Carbohydrate Polymers 2014, 111, 288-297.

13 A. Sionkowska, A. Płanecka, Journal of Molecular Liquids., 2013, 178, 5-14.

14 J. He, Y. Liu, X. Hao, M. Mao, L. Zhu, D. Li, Materials Letters., 2012, 78, 102-105.

15 N. Sawatjui, T. Damrongrungruang, W. Leeanansaksiri, P. Jearanaikoon, T. Limpaiboon, Materials Letters., 2014, 126, 207-210.

16 Y. Zhou, H. Yang, X. Liu, J. Mao, S. Gu, W. Xu, International Journal of Biological Macromolecules., 2013, 53, 88-92.

17 P. Agrawal, G.J. strijkers and K. nicolay, Advanced drug delivery reviews., 2010, 62, 42-58.

18 N. Bhattarai, J. gunn and M.Q. zhang, Advanced drug delivery reviews., 2010, 62, 83-99.

19 T. Kean and M. Thanou, Advanced drug delivery reviews., 2010, 62, 3-11.

20 L.L. Hench and J. Wilson, An Introduction to Bioceramics, World Scientific, Singapore, 1993, pp. 3–5.

21 L.L. Hench, Bioceramics: from concept to clinic, J. Am. Ceram. Soc., 1991, 74 (7), 1487.

22 R. Bermejo, Y. Torres, M. Anglada, L. Llanes, J. Am. Ceram. Soc., 2008, 91, 1618–1625.

23 S.M. Olhero, I. Ganesh, P.M.C. Torres, J. Am. Ceram. Soc., 2009, 92, 9–16.

24 E. Verné, C.V. Brovarone, C. Moisescu, E. Ghisolfi, E. Marmo, Acta Materialia.,2000, 48, 4667-4671.

25 H.S. Costa, A.A.P. Mansur, E.F. Barbosa-Stancioli, M.M. Pereira, H.S. Mansur, J. Mater. Sci. 2008, 43(2), 510-24.

26 S. Bose, J. Darsell, H.L. Hosick, L.H. Yang, D.K. Sarkar, A. Bandyopadhyay, J. Mater. Sci. Mater. Med., 2002, 13, 23-28.

27 X. Miao, Y. Hu, J. Liu, X. Huang, Mat. Sci. Eng. C, Biomim. 2007, 27(2), 257-61.

28 D. Rokusek, A. Bandyopadhyay, S. Bose, H.L. Hosick, J. Biomed. Mater. Res., 2005, 75A, 588.

29 Y. Song, Y. Ju, Y. Morita, B. Xu, G. Song, Materials Science and Engineering., 2014, C 37, 120–126.

30 A. Chanda, R.S Roy, W. Xue, S. Bose, A. Bandyopadhyay, Materials Science and Engineering., 2009, C 29, 1201–1206.

31 F.S. Shirazi, M. Mehrali, A.A. Oshkour, H.S.C. Metselaar, N.A. Kadri, N.A.A. Osman, J. Mech Behav Biomed. 2014, 30, 168–175.

32 I. Sopyan, A. Fadli, M. Mel, J. Mech Behav Biomed. 2012, 8, 86–98.

33 L. Ghorbanian, R. Emadi, S.M. Razavi, H. Shin and A. Teimouri, International Journal of Biological Macromolecules., 2013, 58, 275– 280.

34 A. Teimouri, L. Ghorbanian, A.R. Najafi Chermahini and R. Emadi, Ceramics International., 2014, 40, 6405–6411.

35 D.N. Rockwood, R.C. Preda, T. Yucel, Wang Xiaoqin, M.L. Lovett and D.L. Kaplan, Nature protocols., 2011, 10, 1612-1631.

36 R. Nazarov, H.J. Jin and D.L. Kaplan, Biomacromolecules., 2004, 5, 718-726.

37 T. Kokubo and H. Takadama, Biomaterials., 2006, 27,2907–2915.

38 S.H. Kim, Y.S. Nam, T.S. Lee and W.H. Park, Polymer Journal., 2003, 35, 185–190.

39 B.B. Mandal and S.C. Kundu, Biotechnol Bioeng., 2008, 100, 1237–1250.

40 I.C. Um, H.Y. Kweon, Y.H. Park and S. Hudson, Int J Biol Macromol., 2001, 29, 91–97.

41 U.J. Kim, J. Park, H. Joo Kim, M. Wada and D.L. Kaplan, Biomaterials., 2005, 26, 2775–2785.

42 J. Li, Y. Dou, J. Yang, Y. Yin, H. Zhang, F. Yao, H. Wang and Y. Yao, Mater. Sci. Eng., 2009, 29, 1207–1215.

43 S. A. Hosseini., A. Niaei and D. Salari Open J. of Phys. Chem., 2011, 1, 23–27.

44 M. Peter, N.S. Binulal, S.V. Nair, N. Selvamurugan, H. Tamura and R. Jayakumar, Chem. Eng. J., 2010, 158, 353–361.

45 S. Zmora, R. Glicklis and S. Cohen, Biomaterials., 2002, 23, 4087–4094.

46 M.H. Ho, P.Y. Kuo, H.J. Hsieh, T.Y. Hsien, L.T. Hou, J.Y. Lai and D.M. Wang, Biomaterials., 2004, 25, 129–138.

47 J. Zeltinger, J.K. Sherwood, D.A. Graham, R. Mueller and L.G. Griffith, Tissue Eng. 7 2001, 7, 557–572.

48 S.J. Hollister, Nat. Mater., 2005, 4, 518–524.

49 S.B. Bahrami, Iranian polymer., 2003, 12, 139-146.

50 E. Peon, G. Fuentes, JA. Delgado, L. Morejon, A. Almirall and R. Garcia, LAAR., 2004, 34, 225-228.

51 F. Grinnell, C.H. Ho, Y.C. Lin and G. Skuta, J. Biol. Chem. 274 (1999) 918–923.

52 S.R. Peyton and A.J. Putnam, J. Cell Physiol., 2005, 204, 198–209.

53 B. Harley, H.D. Kim, M.H. Zaman, I.V. Yannas, D.A. Lauffenburger and L.J. Gibson, Biophys. J., 2008, 95, 4013–4024.

54 R. Nazarov, H.J. Jin, D.L. Kaplan, Biomacromolecules., 2004, 5, 718-726.

55 U.J. Kim, J. Park, H.J. Kim, M. Wada and D.L. Kaplan, Biomaterials., 2005, 26, 2775–2785.

37

56 L. J. Gibson and M.F. Ashby, Cellular solids-structure and properties. Second edition ed. 1999: Cambridge Solid State Science Series, Cambridge University Press.

Fabrication and characterization of silk fibroin/chitosan/Nano γ-alumina composite scaffolds for tissue engineering applications

Abbas Teimouri[a,*], Raheleh. Ebrahimi[a], Rahmatollah Emadi[b], Alireza Najafi Chermahini[c]

[a] *Chemistry Department, Payame Noor University, 19395-3697, Tehran, I. R. of Iran*
[b] *Department of Materials Engineering, Isfahan University of Technology, Isfahan 84156-83111, Iran*
[c] *Department of Chemistry, Isfahan University of Technology, Isfahan, 841543111, Iran*

A series of silk fibroin/chitosan/Nano γ-alumina composite scaffolds have been prepared using the lyophilization technique for tissue engineering. These were then characterized using SEM, XRD, EDX, FTIR and TGA. In addition, the water uptake capacity, degradability, and biomineralization capability of the composite scaffolds were assessed. The inclusion of γ-alumina in the SF/CS γ-alumina scaffolds was found to result in increased compressive strength and water uptake capacity and decreased porosity. Cytocompatibility of the scaffolds was also assessed by MTT assay and cell attachment studies using Human Gingival Fibroblast cells (HGF, NCBI: C-131). Results showed no signs of toxicity and cells were found attached to the pore walls within the scaffolds. These results proposed that the developed composite scaffolds meet the requirements for tissue engineering applications.

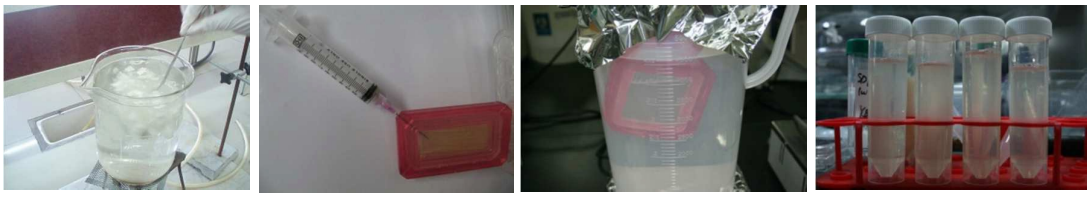

*Corresponding author at: Department of Chemistry, Payame Noor University (PNU), Isfahan, P.O. Box 81395-671, Iran. Tel.: +98 31 33521804; fax: +98 31 33521802.
E-mail addresses: a teimouri@pnu.ac.ir, a teimoory@yahoo.com (A. Teimouri).